# Imaging and radiation therapy: Current trends and future possibilities

Monica Shukla, MD, Aryavarta Kumar, MD, PhD, Andrew Godley, PhD, and Deepak Khuntia, MD

W e have seen a tremendous boom in medical imaging use from the diagnostic side, but over the last decade, the technology has shown increased utilization in the therapeutic delivery of radiation. In this review, we summarize medical imaging's current role and future possibilities in both the planning and delivery of therapeutic radiation.

## Imaging in treatment planning
### Fluoroscopy and computed tomography

Early radiotherapy planning was based on body surface landmarks alone. Conventional or fluoroscopic simulation acquires 2-dimensional (2D) images for radiotherapy planning based on internal anatomic landmarks and limited tissue-density information. Computed axial tomography (CT) became available in the 1970s, but the developments in computer processing

*Dr. Shukla is a PGY-4 Radiation Oncology Resident, Dr. Kumar is a Radiation Oncology Resident, and Dr. Godley is a Physicist, Department of Radiation Oncology, Cleveland Clinic Foundation, Cleveland, OH; and Dr. Khuntia is a Radiation Oncologist and President at Spectrum Physics Corporation, Los Altos, CA.*
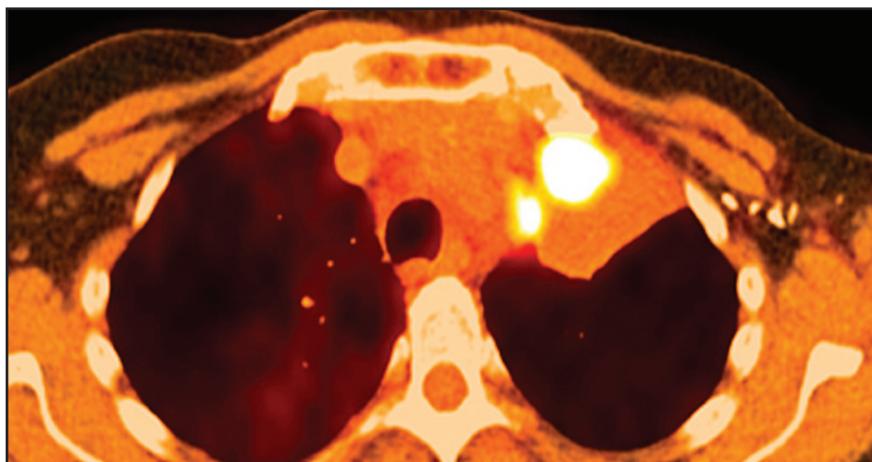
speed, memory, and applications specifically for use in radiotherapy did not allow CT simulation to become feasible until the late 1990s.[1] To compare traditional to modern techniques, a study was conducted of 30 patients whose cancer treatments were planned with surface markings, fluoroscopy, and CT simulation.[2] The authors showed that CT simulation increased the dose to the target and reduced the dose to surrounding normal structures more significantly than the older technologies using surface markers and fluoroscopy. The current standard in most countries is CT-simulator-based treatment planning for optimal coverage of target volumes and sparing of normal structures,

although fluoroscopy simulation is still widely used in developing countries.

### Magnetic resonance imaging

Magnetic resonance imaging (MRI) is a valuable cross-sectional imaging modality known for its superior soft-tissue delineation as compared to CT. Images are produced based on the interaction between hydrogen nuclei within tissues and a large external magnetic field, as well as radiofrequency bursts, which manipulate the spin of the hydrogen nuclei. Image acquisition parameters can be modified to enhance tumor characteristics (vascularity, extent of infiltration, peritumoral edema, etc). MRI is routinely used in treatment planning for primary and
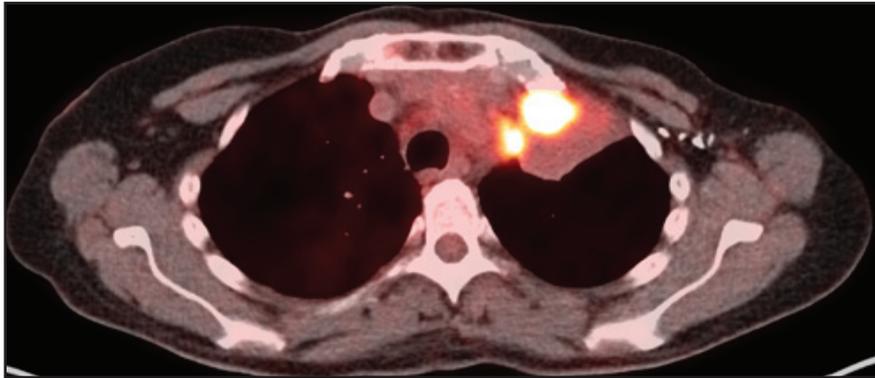
**FIGURE 1.** *FDG PET/CT image of a 55-year-old female with stage IIIA NSCLC. There is a hypermetabolic lesion in her left upper lobe, max SUV 18.3. The mass is compressing her left bronchus (not shown), resulting in an adjacent soft-tissue density consistent with left upper-lobe collapse. PET nicely differentiates tumor mass from atelectasis.*

secondary tumors of the brain and spine.[3] It allows better visualization of lesions near bone and is particularly helpful in diagnosing and treating lesions in the posterior fossa. For brain metastases, MRI is much more sensitive than CT, particularly at identifying small lesions (≤ 0.5 cm).[4] The ability to visualize these lesions prevents patients from aggressive definitive-intent local therapies and also allows these lesions to be targeted by techniques such as stereotactic radiosurgery, which can be delivered with submillimeter accuracy. Additionally, MRI is used for treatment planning in gastrointestinal,[5] genitourinary,[6] head and neck,[7] gynecologic,[8] and sarcomatous tumors[3] because its high soft-tissue contrast allows the assessment of extent and spread of disease, which ultimately influences radiation treatment volumes. One drawback of MRI for radiation planning is that it lacks the electron density information required for calculating photon attenuation so co-registration with a CT is usually required for planning purposes.

### Positron emission tomography

Positron emission tomography (PET) is a type of molecular imaging that allows measurement of a metabolic process within tissues. In PET, the subject is injected with a radioactive isotope (eg, fluorodeoxyglucose, ^{18}F-FDG), which undergoes positron decay. The positron emitted travels for a short distance within tissues and interacts with an electron. Both particles are annihilated and produce a pair of 511-keV gamma photons, emitted 180 degrees apart. Photon pairs are collected and can be localized to point source within the tissue.[9] PET scans are co-registered to CT scans, which provide detailed anatomic information. Ideally, a PET scan is done at the time of CT simulation with the patient in the planned treatment position. If integrated PET/CT simulation is not available, a PET scan can be done at a later date with the patients positioned in their custom-created immobilization device. A common but less ideal scenario is when a diagnostic PET scan and a CT simulation are done in different positions. In this case, both sets of images are coregistered or "fused" as closely as possible.[10]

PET can add several key pieces of information for the radiation oncologist. PET often identifies targets not easily visualized on CT or MRI, such as satellite tumor lesions and lymph node metastases, which would alter radiation treatment volumes. It also allows exclusion of targets that appear ambiguous on CT, but are, with fair certainty, negative on PET. PET also allows alteration of radiation volumes and doses based on response to other antineoplastic therapies, such as in lymphoma treatment.[10]

^{18}F-FDG is the most commonly used radiotracer in combination with PET. ^{18}F-FDG is a glucose analogue taken up by cells via glucose transporters. After entering the cell, ^{18}F-FDG is phosphoryated by an enzyme called hexokinase, resulting in the molecule being trapped within cells. FDG accumulates in tissues with high cellular activity requiring increased glucose uptake and consumption. Particularly upregulated in tumor cells is the inefficient glycolytic pathway that is preferentially used for ATP generation.[11] ^{18}F-FDG uptake is not specific for tumor cells; it also localizes within inflamed and infected tissues that are also metabolically active and depend heavily on the glycolysis pathway.

Since the mid-1990's, several studies have shown that ^{18}F-FDG -PET increases the sensitivity and specificity of CT to properly stage cancers locally, regionally, and distantly. As such, PET often saves patients from unnecessary surgery or other aggressive treatments[12] and increases the accuracy of locoregional therapies. Several ^{18}F-FDG-PET studies were evaluated against standard imaging modalities, such as x-ray and CT for the definition of radiation treatment volumes. Use of FDG-PET in the target volume definition has been best studied in nonsmall cell lung cancer. On the whole, these studies suggest ^{18}F-FDG-PET can influence the definition of the gross target volume (GTV) in most cases[13-16] Particularly helpful in NSCLC lung cancer is PET's ability to discern atelectatic lung tissue from tumor mass and, with a higher sensitivity, to detect lymph-node metastases in the chest (Figure 1).[17-20] The main drawback of PET is its limited resolution for detecting tumors or lymph nodes with a diameter < 1 cm , unless the SUV is at least 4 times background levels.[10] Another area of controversy is the definition of the edge of the PET tumor volume, as the volume is greatly affected by windowing and thresholding.[21,22] For this reason, protocols must
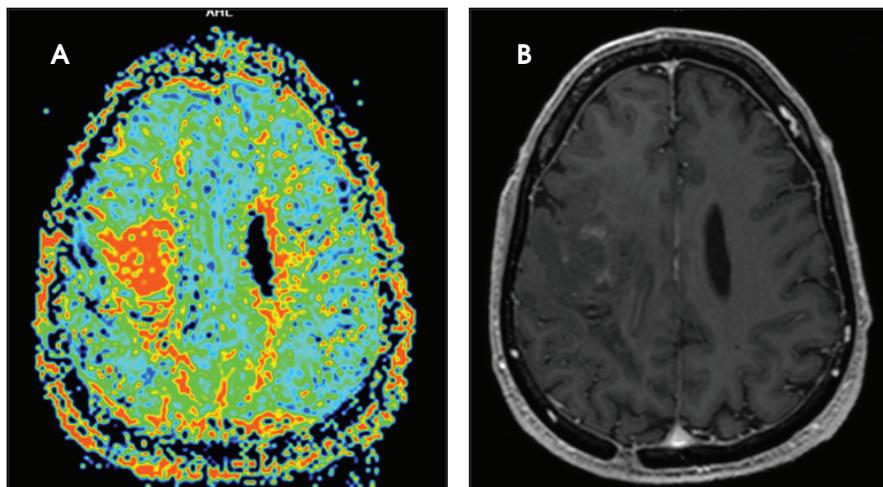
# CME



**FIGURE 2.** *This is a 54-year-old male (A) with a right frontal low-grade astrocytoma noted to have accelerated progression of the tumor 17 years after initial diagnosis. MRI (B) with contrast (bottom image) shows increased patchy enhancement in the right frontotemporal mass. There is increased CBV in the same area with a rough relative CBV ratio of 3.0:3.5, compared to the contralateral cerebral white matter indicating tumor progression (top image).*

use a clearly defined process for contouring tumors based on PET information. The most recent phase III NSCLC RTOG protocol 0617 recommended, but did not require, PET for planning purposes. If PET was used, tissues with a pretreatment SUV of > 3 were included in the GTV. Just as in NSCLC, PET is more sensitive than CT alone for detection of lymph node metastases in head and neck cancers, which is critical for dose and volume determination.[23] The specificity of PET, however, is reduced, as it will also detect inflammatory processes in lymph nodes and other lymphatic tissues. Also critical in treatment of head and neck cancers is the need for the planning PET to be done in the treatment position so that CT and PET targets match.[24] PET is also regularly used in diagnosis and treatment planning for SCLC,[25] esophageal cancer,[26,27] and lymphoma.[28,29]

## Future trends
### *Dynamic contrast-enhanced CT/MRI*

Dynamic contrast-enhanced (DCE) CT and MRI imaging allows visualization of vasculature within tumors and surrounding tissues. Vascular proper-ties that can be examined include blood flow, blood volume, and permeability.[30] Blood vessels formed in angiogenesis are imperfect, displaying tortuosity and high permeability. In malignant gliomas, cerebral blood volume (CBV) and permeability assessed by DCE are consistently linked to worse outcomes. Several studies have related high-tumor CBV or a fraction of the tumor volume that has a high CBV with a shorter time to progression and worse overall survival (Figure 2).[31,32] CBV has been used during a course of RT to assess early treatment response.[33] With this information, additional radiation dose can be targeted to those to areas, which appear to have more neovascularization, indicating high tumor activity and aggressiveness. Despite neovascularization, areas of the tumor may still be inadequately perfused and hypoxic due to the poorly functioning nature of these vessels. Hypoxic tumors are more resistant to radiotherapy.[11] Several studies investigated DCE-MRI to identify poorly enhancing tumors, indicating areas of hypoxia that may be resistant to radiotherapy. A study in cervical cancer showed local control and overall survival were better in those with minimal areas of poor enhancement versus those patients with large areas of enhancement.[34] Similar studies have been done in SCC of the head and neck, relating poor tumor perfusion as assessed by DCE-CT/MRI with increased local recurrence.[35,36] The barrier to widespread use of DCE imaging is the lack of standardized imaging protocols that specify parameters for image acquisition, quantification of the results, and quality control for reproducibility and accuracy of the acquired images.[30] Several efforts are under way to address these technical issues and despite these hurdles, DCE imaging is currently being evaluated in over 40 clinical studies in the United States.

### *18F-fluorothymidine PET (FLT-PET)*

The nonspecificity of FDG-PET for cancer cells has led to interest in other radiotracers such as 3′-deoxy-3′-[(18)F]fluorothymidine (FLT). FLT is selectively taken up by proliferating cells via various nucleoside transporters to be used in the pyrimidine salvage pathway, which is upregulated in the S-phase. After entering the cell, it is phosphylated by thymidine kinase 1 (TK1), trapping it within the cell.[37] Pathologically, FLT uptake has been correlated with rate of cellular proliferation, and markers thereof such as Ki-67.[38] An advantage that FLT has over FDG is the specificity for identifying actively replicating tissue. As mentioned above, FDG is not specific for proliferating tissues and is often taken up by normal tissue, leading to more false-positives. However, the converse of that is also true with FLT in some series, leading to more false-negative results. One particular example is if a tumor cell switches to synthesizing pyrimidines bases de novo, and not via the salvage pathway, FLT will not be taken up by actively dividing cells.[37] Despite these caveats, FLT is still a promising radiotracer being evaluated in several body sites for assessment to treatment response. Several studies have shown that FLT
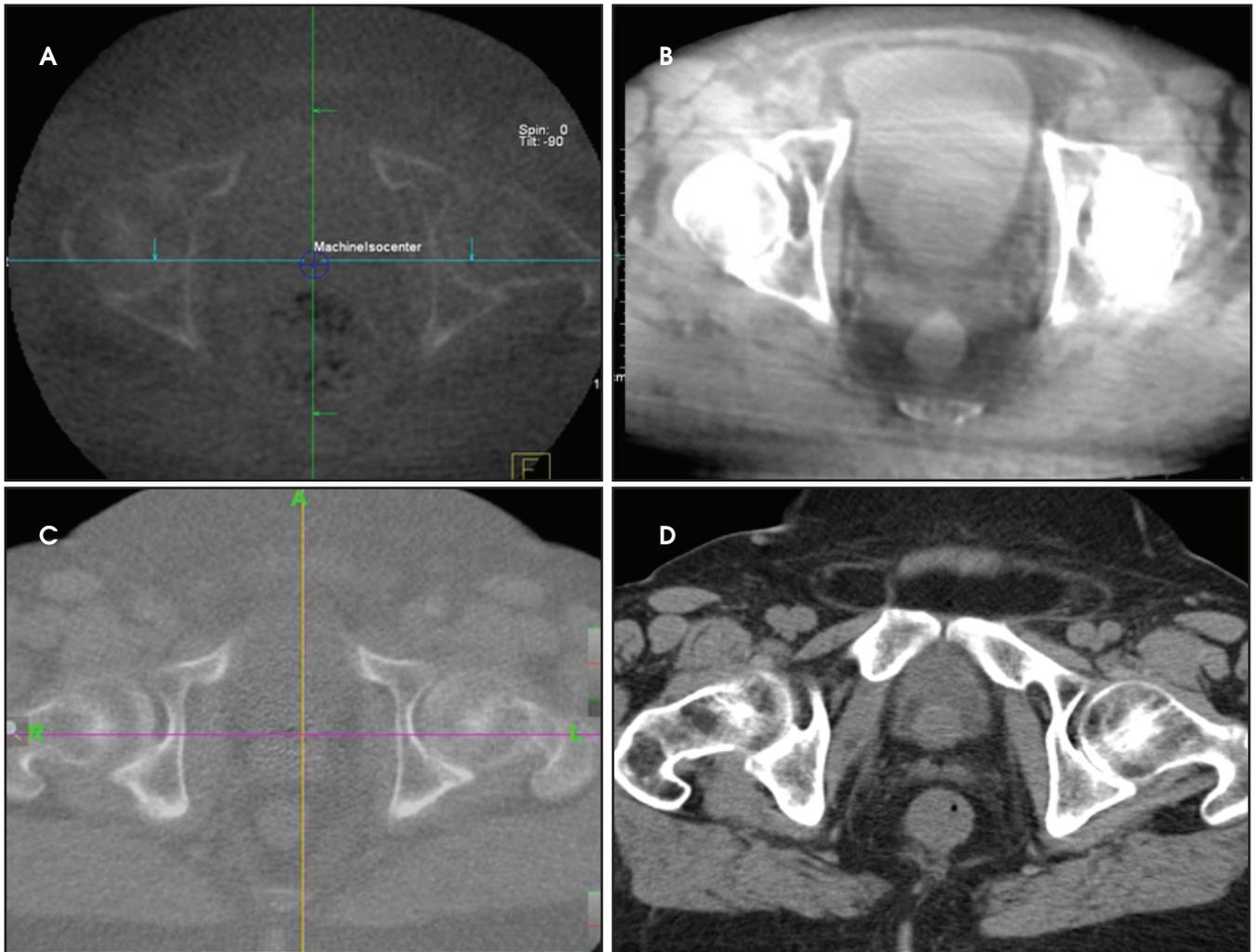
**FIGURE 3.** IGRT image quality comparison. Clockwise from top left, MV CBCT (A), kV CBCT (B), kV FBCT (C), and MV FBCT (D) axial slice of separate prostate patients. MV images courtesy of N. Morrow, Medical College of Wisconsin, Milwaukee, WI.

uptake declines earlier and more significantly than does FDG uptake. This has been shown following single-fraction radiotherapy in vitro, as well as in experimental models of esophageal carcinoma following docetaxel plus radiation.[39,40] Clinically, the level of FLT uptake reduction has been correlated to partial and complete response to chemotherapy in non-Hodgkin's lymphoma patients.[41] In oropharyngeal cancer patients, FLT showed a two-fold decrease in uptake in the first 2 weeks after initiation of RT and another two-fold decrease by week 4 into treatment. Due to the early response, the authors of this study proposed that the tumor subvolume with continued

^{18}F-FLT uptake could be selectively targeted with increased radiation dose.[42]

## Copper(II)-diacetyl-bis(N4-methylthiosemicarbazone) PET (Cu-ATSM PET)

Tumors are heterogeneous populations known to contain hypoxic areas. Hypoxia stimulates angiogenesis and tumor progression and also confers resistance to tumor directed therapies.[43] With radiation therapy in particular, several studies have shown that dose-escalation may be one way to overcome this resistance to therapy.[11] Cu(II)-diacetyl-bis($N^4$-methylthiosemicarbazone (Cu-ATSM) is a radiotracer that

can identify hypoxic areas within tumor cells potentially allowing clinicians an opportunity to intensify local therapy to these areas.[44] Cu-ATSM was first reported in 1997 as a copper chelate that localized within ischemic cardiac myocytes while washing out of normoxic muscle.[45] Several early animal studies confirmed that ATSM accumulation was dependent on tumor oxygen tension.[46] Chao et al demonstrated the feasibility of using coregistered CT and CuATSM PET images to create an hGTV or a hypoxic tumor subvolume for selective dose escalation in a patient with node positive SCC of the right tonsil/BOT.[47] Since then, Cu-ATSM

# CME

**Table 1. Summary and comparison of IGRT techniques. Time includes the execution of both imaging and registration. Residual error, which reflects the relative accuracy of the modality, is calculated for breast in optical tracking, external markers for IR tracking, and prostate for all others.**

| Modality | Dose (cGy) | Time (min) | Residual error (mm) | Real-time | Notes | Examples |
|---|---|---|---|---|---|---|
| Ultrasound | NA | 5-10 | 6 | In development | User dependent, transducer can distort anatomy being imaged | Clarity, BAT, SonArray |
| MV Planar | 1-5 | 2-4 | 5 | In development | Potential exit dose measurement, treatment delivery verification | EPIDs |
| kV Planar | 0.1-0.5 | 1-2 | 1.5 | Yes | Imaging planes at 45° to orthogonal | Exactrac, Cyberknife |
| MV CBCT | 5-20 | 4-6 | 4.5 | No | Common isocenter, low soft-tissue resolution | Mvision |
| kV CBCT | 1-3 | 4-6 | 3 | No | No common isocenter, good soft-tissue resolution | XVI, OBI |
| MV CT | 1-2 | 4-7 | 4 | No | Reduced metal artifacts | TomoTherapy |
| kV CT | 1-3 | 5-8 | 2.5 | No | Needs markers to transfer treatment isocenter to CT | CTVision, ExaCT |
| IR tracking | NA | 0.5-1 | 0.5 | Yes | Registration of external surrogates not target | ExacTrac, DynaTrac, Cyberknife |
| Optical | NA | 0.5-1 | 3 | Yes | Skin needs to be visible, matches surface | AlignRT |
| RF tracking | NA | 3-5 | 1.5 | Yes | Requires implanted fiducials, special couchtop | Calypso, MicroPos |
| MRI | NA | 1-10 | — | In development | Special accelerator and treatment room | ViewRay, MRI-on-Rails |

uptake has been studied as a predictor of response to chemoradiotherapy in several body sites, including the rectum,[48] cervix,[49,50] and head and neck.[51] One study in locally advanced head and neck cancer found that at 2 years post-chemoradiotherapy, pretreatment SUV max on Cu-ATSM PET/CT differed significantly between those patients that remained NED and those that had recurrent or residual disease, suggesting that the degree of pretreatment Cu-ATSM uptake is predictive of response to definitive chemoRT. No significant difference was seen between these two groups on FDG-PET.[52] Cu-ATSM is a promising radiotracer and is currently the subject of several pilot studies to assess its utility in NSCLC, brain metastases, head and neck cancer, prostate cancer, and esophageal cancer.

## Imaging during treatment

The goal of image guidance during radiotherapy is to ensure proper targeting and delivery of radiation. Radiation planning, margins, and patient immobilization setups are very important and work alongside image-guided radiation therapy (IGRT) to assist with proper delivery.[53] Table 1 summarizes differences between IGRT techniques.

## IGRT using ionizing radiation

Megavoltage (MV) and kilovoltage (kV) photon imaging are commonly used in today's radiation oncology practices.[54,55] Traditionally, port films were used to verify anatomic setup and were later replaced by electronic portal image devices (EPIDs) as quick snapshots of patient position and field shape that utilized low doses of MV radiation. These images represent a 2D projection of a patient with poor soft-tissue resolution. To improve on this, tomography technology was developed to help with 3D IGRT, and kV imaging was introduced to help with soft-tissue resolution.

Peripheral kV imaging improves the contrast of anatomy over MV due to the larger range of attenuation of kV photons in tissue. However kV systems require accurate calibration to the treatment isocenter. For 3D imaging, cone-beam CT (CBCT) is reconstructed using a 'cone' of photons rotating around the patient, imaging an entire 10- to 30-cm section at once, while in conventional CT, the 3D image is formed by translating the patient and imaging only a few slices at a time with a 'fan' beam (FBCT). Due to the large width of the cone beam used to image the patient, considerable photon scatter degrades the CBCT image compared to the conventional CT image. The CBCT technologies can have energies in the kV or MV range with the caveat that kV technology is a peripheral imaging device. Tomotherapy (Accuray Inc, Sunnyvale, CA) uses a narrow fan beam for imaging, but with MV photons. For the best image quality, CT on rails places a diagnostic CT scanner in the treatment vault.[55-57] The difference between mega- and kilo-volt and cone- and fanbeam is illustrated in Figure 3. It should be noted that choice of IGRT depends on the target and surrounding structures. For example, the most efficient IGRT for a tumor adjacent to the vertebral column would be a plain film, however, an intraabdominal tumor surrounded by soft tissue would benefit the most from CT-based imaging.

### IGRT using nonionizing energies

Sonography is a common IGRT modality requiring a probe in the appropriate position to aid setup before treatment commences. These images can be combined with CT-based imaging to help visualize the target. Real-time sonography with the transducer held in place by a robot during treatment is under development. In general, sonography provides the lowest resolution of IGRT and does have a learning curve, but is easy to set up, reduces the patient's exposure to ionizing radiation seen with other IGRT modalities, and clinically, it has been used in breast and prostate radiotherapy treatments.[58] Infrared (IR) tracking uses external reflective markers either directly on the patient, or on a stereotactic frame, as a proxy to track target motion. Similarly, optical tracking matches surface anatomy and so is limited to treatment regions close to the surface, such as in the breast. Radiofrequency targeting, such as Calypso (Varian Medical Systems, Palo Alto, CA), offers a method for real-time tracking and is FDA approved for use in prostate cancer patients[59] and was recently approved for use with skin-based fiducial markers.

MRI-based systems could offer the next step to increasing soft-tissue delineation. Technological challenges are being worked out, including the interference between the RF signals from the MRI coils and the RF pulses from the electron acceleration in the linac and the magnetic field's disruption of the treatment beam. ViewRay (View Ray, Inc., Cleveland, OH) has a product that uses 3 Co-60 teletherapy units and a split-magnet MRI system to offer real-time imaging during treatment. These systems are being constructed in a few centers in the United States. Other technology, such as PET-based IGRT, is currently under development.

### Conclusion

We have summarized the current use of imaging in radiation oncology. As technology has evolved on the hardware side, there is a growing desire to increase the therapeutic ratio on the radiation delivery side of cancer care. We are now able to deliver radiation to submillimeter accuracy, further sparing normal tissues beyond what has ever been done before. Further, there has been a growing trend to hypofractionate (reducing the number of treatments while increasing the dose per treatment). This growing demand has resulted in a higher demand for imaging in daily radiation practices.

The future of imaging in radiotherapy also is exciting. As coined by Bentzen, the new field of "theragnostics" in radiotherapy that is in its infancy.[60] With the advent of theragnostics, advanced imaging techniques, such as FLT-PET, DCE CT/MRI, and Cu-ATSM imaging, may allow us to tailor our radiotherapy based on the response to initial chemotherapy and radiation treatment, further enhancing our ability to improve the therapeutic ratio.

### REFERENCES

1. Aird EG, Conway J. CT simulation for radiotherapy treatment planning. *Br J Radiol.*2002;75:937-949.
2. Suhag V, Kaushal V, Yadav R, Das BP. Comparison of simulator-CT versus simulator fluoroscopy versus surface marking based radiation treatment planning: a prospective study by three-dimensional evaluation. *Radiother Oncol.* Jan 2006;78:84-90.
3. Khoo VS. MRI—"magic radiotherapy imaging" for treatment planning? *Br J Radiol.* 2000;73:229-233.
4. Akeson P, Larsson EM, Kristoffersen DT, Jonsson E, Holtas S. Brain metastases—comparison of gadodiamide injection-enhanced MR imaging at standard and high dose, contrast-enhanced CT and non-contrast-enhanced MR imaging. *Acta Radiol.* 1995;36:300-306.
5. O'Neill BDP, Salerno G, Thomas K, Tait DM, Brown G. MR vs CT imaging: low rectal cancer tumour delineation for three-dimensional conformal radiotherapy. *Brit J Radiol.* 2009;82:509-513.
6. Chen L, Price RA, Jr., Wang L, et al. MRI-based treatment planning for radiotherapy: dosimetric verification for prostate IMRT. *Int J Radiat Oncol Biol Phys.* 2004;60:636-647.
7. Newbold K, Partridge M, Cook G, et al. Advanced imaging applied to radiotherapy planning in head and neck cancer: a clinical review. *Br J Radiol.* 2006;79:554-561.
8. Barillot I, Reynaud-Bougnoux A. The use of MRI in planning radiotherapy for gynaecological tumours. *Cancer Imaging.* 2006;6:100-106.
9. Khan FM. *The physics of radiation therapy.* 4th ed. Philadelphia, PA: Lippincott Williams & Wilkins; 2010.
10. Belohlavek O, Carrio I, Danna M, et al. *The Role of PET/CT in Radiation Treatment Planning for Cancer Patient Treatment.* Vienna: IAEA; 2008.
11. Hall EJ, Giaccia AJ. *Radiobiology for the radiologist.* 7th ed. Philadelphia: Wolters Kluwer Health/Lippincott Williams & Wilkins; 2012.
12. van Tinteren H, Hoekstra OS, Smit EF, et al. Effectiveness of positron emission tomography in the preoperative assessment of patients with suspected non-small-cell lung cancer: the PLUS multicentre randomised trial. *Lancet.* 2002;359:1388-1393.
13. Erdi YE, Rosenzweig K, Erdi AK, et al. Radiotherapy treatment planning for patients with non-small cell lung cancer using positron emission tomography (PET). *Radiother Oncol.* 2002;62:51-60.

# CME

14. Messa C, Ceresoli GL, Rizzo G, et al. Feasibility of [18F]FDG-PET and coregistered CT on clinical target volume definition of advanced non-small cell lung cancer. *Q J Nucl Med Mol Imaging.* 2005;49:259-266.

15. Kiffer JD, Berlangieri SU, Scott AM, et al. The contribution of 18F-fluoro-2-deoxy-glucose positron emission tomographic imaging to radiotherapy planning in lung cancer. *Lung Cancer.* 1998;19:167-177.

16. Mac Manus MP, Hicks RJ, Matthews JP, et al. Positron emission tomography is superior to computed tomography scanning for response-assessment after radical radiotherapy or chemoradiotherapy in patients with non-small-cell lung cancer. *J Clin Oncol.* 2003;21:1285-1292.

17. Graeter TP, Hellwig D, Hoffmann K, et al. Mediastinal lymph node staging in suspected lung cancer: comparison of positron emission tomography with F-18-fluorodeoxyglucose and mediastinoscopy. *Ann Thorac Surg.* 2003;75:231-235; discussion 235-236.

18. Dwamena BA, Sonnad SS, Angobaldo JO, Wahl RL. Metastases from non-small cell lung cancer: mediastinal staging in the 1990s--meta-analytic comparison of PET and CT. *Radiology.* 1999;213:530-536.

19. Nestle U, Schaefer-Schuler A, Kremp S, et al. Target volume definition for 18F-FDG PET-positive lymph nodes in radiotherapy of patients with non-small cell lung cancer. *Eur J Nucl Med Mol Imaging.* 2007;34:453-462.

20. Vanuytsel LJ, Vansteenkiste JF, Stroobants SG, et al. The impact of (18)F-fluoro-2-deoxy-D-glucose positron emission tomography (FDG-PET) lymph node staging on the radiation treatment volumes in patients with non-small cell lung cancer. *Radiother Oncol.* 2000;55:317-324.

21. Yaremko B, Riauka T, Robinson D, et al. Threshold modification for tumour imaging in non-small-cell lung cancer using positron emission tomography. *Nucl Med Commun.* 2005;26:433-440.

22. Hong R, Halama J, Bova D, et al. Correlation of PET standard uptake value and CT window-level thresholds for target delineation in CT-based radiation treatment planning. *Int J Radiat Oncol Biol Phys.* 2007;67:720-726.

23. Paulino AC, Koshy M, Howell R, et al. Comparison of CT- and FDG-PET-defined gross tumor volume in intensity-modulated radiotherapy for head-and-neck cancer. *Int J Radiat Oncol Biol Phys.* 2005;61:1385-1392.

24. Wang D, Schultz CJ, Jursinic PA, et al. Initial experience of FDG-PET/CT guided IMRT of head-and-neck carcinoma. *Int J Radiat Oncol Biol Phys.* 2006;65:143-151.

25. Kamel EM, Zwahlen D, Wyss MT, et al. Whole-body (18)F-FDG PET improves the management of patients with small cell lung cancer. *J Nucl Med.* 2003;44:1911-1917.

26. Leong T, Everitt C, Yuen K, et al. A prospective study to evaluate the impact of FDG-PET on CT-based radiotherapy treatment planning for oesophageal cancer. *Radiother Oncol.* 2006;78:254-261.

27. Moureau-Zabotto L, Touboul E, Lerouge D, et al. Impact of CT and 18F-deoxyglucose positron emission tomography image fusion for conformal radiotherapy in esophageal carcinoma. *Int J Radiat Oncol Biol Phys.* 2005;63:340-345.

28. Yahalom J. Transformation in the use of radiation therapy of Hodgkin lymphoma: new concepts and indications lead to modern field design and are assisted by PET imaging and intensity modulated radiation therapy (IMRT). *Eur J Haematol Suppl.* 2005:90-97.

29. Hutchings M, Loft A, Hansen M, et al. Clinical impact of FDG-PET/CT in the planning of radiotherapy for early-stage Hodgkin lymphoma. *Eur J Haematol.* 2007;78:206-212.

30. Cao Y. The promise of dynamic contrast-enhanced imaging in radiation therapy. *Semin Radiat Oncol.* 2011;21:147-156.

31. Wong ET, Jackson EF, Hess KR, et al. Correlation between dynamic MRI and outcome in patients with malignant gliomas. *Neurology.* 1998;50:777-781.

32. Law M, Young RJ, Babb JS, et al. Gliomas: predicting time to progression or survival with cerebral blood volume measurements at dynamic susceptibility-weighted contrast-enhanced perfusion MR imaging. *Radiology.* 2008;247:490-498.

33. Cao Y, Tsien CI, Nagesh V, et al. Survival prediction in high-grade gliomas by MRI perfusion before and during early stage of RT [corrected]. *Int J Radiat Oncol Biol Phys.* 2006;64:876-885.

34. Yamashita Y, Baba T, Baba Y, et al. Dynamic contrast-enhanced MR imaging of uterine cervical cancer: pharmacokinetic analysis with histopathologic correlation and its importance in predicting the outcome of radiation therapy. *Radiology.* 2000;216:803-809.

35. Hermans R, Meijerink M, Van den Bogaert W, et al. Tumor perfusion rate determined noninvasively by dynamic computed tomography predicts outcome in head-and-neck cancer after radiotherapy. *Int J Radiat Oncol Biol Phys.* 2003;57:1351-1356.

36. Hoskin PJ, Saunders MI, Goodchild K, et al. Dynamic contrast enhanced magnetic resonance scanning as a predictor of response to accelerated radiotherapy for advanced head and neck cancer. *Br J Radiol.* 1999;72:1093-1098.

37. Zhang CC, Yan Z, Li W, et al. [(18)F]FLT-PET imaging does not always «light up» proliferating tumor cells. *Clin Cancer Res.* 2012;18:1303-1312.

38. Chalkidou A, Landau DB, Odell EW, et al. Correlation between Ki-67 immunohistochemistry and 18F-Fluorothymidine uptake in patients with cancer: A systematic review and meta-analysis. *Eur J Cancer.* 2012;48:3499-3513.

39. Yang YJ, Ryu JS, Kim SY, et al. Use of 3′-deoxy-3′-[18F]fluorothymidine PET to monitor early responses to radiation therapy in murine SCCVII tumors. *Eur J Nucl Med Mol Imaging.* 2006;33:412-419.

40. Apisarnthanarax S, Alauddin MM, Mourtada F, et al. Early detection of chemoradioresponse in esophageal carcinoma by 3′-deoxy-3′-3H-fluorothymidine using preclinical tumor models. *Clin Cancer Res.* 2006;12:4590-4597.

41. Herrmann K, Wieder HA, Buck AK, et al. Early response assessment using 3′-deoxy-3′-[18F]fluorothymidine-positron emission tomography in high-grade non-Hodgkin's lymphoma. *Clin Cancer Res.* 2007;13:3552-3558.

42. Kishino T, Hoshikawa H, Nishiyama Y, et al. Usefulness of 3′-deoxy-3′-18F-fluorothymidine PET for predicting early response to chemoradiotherapy in head and neck cancer. *J Nucl Med.* 2012;53:1521-1527.

43. Kunz M, Ibrahim SM. Molecular responses to hypoxia in tumor cells. *Mol Cancer.* 2003;2:23.

44. Vavere AL, Lewis JS. Cu-ATSM: A radiopharmaceutical for the PET imaging of hypoxia. *Dalton Trans.* Nov 21 2007(43):4893-4902.

45. Fujibayashi Y, Taniuchi H, Yonekura Y, Ohtani H, Konishi J, Yokoyama A. Copper-62-ATSM: a new hypoxia imaging agent with high membrane permeability and low redox potential. *J Nucl Med.* 1997;38:1155-1160.

46. Takahashi N, Fujibayashi Y, Yonekura Y, et al. Copper-62 ATSM as a hypoxic tissue tracer in myocardial ischemia. *Ann Nucl Med.* 2001;15:293-296.

47. Chao KS, Bosch WR, Mutic S, et al. A novel approach to overcome hypoxic tumor resistance: Cu-ATSM-guided intensity-modulated radiation therapy. *Int J Radiat Oncol Biol Phys.* 2001;49:1171-1182.

48. Dietz DW, Dehdashti F, Grigsby PW, et al. Tumor hypoxia detected by positron emission tomography with 60Cu-ATSM as a predictor of response and survival in patients undergoing Neo-adjuvant chemoradiotherapy for rectal carcinoma: a pilot study. *Dis Colon Rectum.* 2008;51:1641-1648.

49. Dehdashti F, Grigsby PW, Mintun MA, et al. Assessing tumor hypoxia in cervical cancer by positron emission tomography with 60Cu-ATSM: relationship to therapeutic response-a preliminary report. *Int J Radiat Oncol Biol Phys.* 2003;55:1233-1238.

50. Grigsby PW, Malyapa RS, Higashikubo R, et al. Comparison of molecular markers of hypoxia and imaging with (60)Cu-ATSM in cancer of the uterine cervix. *Mol Imaging Biol.* 2007;9:278-283.

51. Kositwattanarerk A, Oh M, Kudo T, et al. Different distribution of (62) Cu ATSM and (18)F-FDG in head and neck cancers. *Clin Nucl Med.* 2012;37:252-257.

52. Minagawa Y, Shizukuishi K, Koike I, et al. Assessment of tumor hypoxia by 62Cu-ATSM PET/CT as a predictor of response in head and neck cancer: a pilot study. *Ann Nucl Med.* 2011;25:339-345.

53. Verhey LJ, Goitein M, McNulty P, et al. Precise positioning of patients for radiation therapy. *Int J Radiat Oncol Biol Phys.* 1982;8:289-294.

54. Shiu AS, Hogstrom KR, Janjan NA, et al. Technique for verifying treatment fields using portal images with diagnostic quality. *Int J Radiat Oncol Biol Phys.* 1987;13:1589-1594.

55. Morrow NV, Lawton CA, Qi XS, Li XA. Impact of computed tomography image quality on image-guided radiation therapy based on soft tissue registration. *Int J Radiat Oncol Biol Phys.* 2012;82:e733-738.

56. Morin O, Gillis A, Chen J, et al. Megavoltage cone-beam CT: System description and clinical applications. *Med Dosim.* 2006;31:51-61.

57. Court L, Rosen I, Mohan R, Dong L. Evaluation of mechanical precision and alignment uncertainties for an integrated CT/LINAC system. *Med Phys.* 2003;30:1198-1210.

58. Chadha M, Young A, Geraghty C, et al. Image guidance using 3D-ultrasound (3D-US) for daily positioning of lumpectomy cavity for boost irradiation. *Radiat Oncol.* 2011;6:45.

59. Willoughby TR, Kupelian PA, Pouliot J, et al. Target localization and real-time tracking using the Calypso 4D localization system in patients with localized prostate cancer. *Int J Radiat Oncol Biol Phys.* 2006;65:528-534.

60. Bentzen SM. Theragnostic imaging for radiation oncology: dose-painting by numbers. *Lancet Oncol.* 2005;6:112-117.